Quantum Chemical Study on the Configurations of Encapsulated Metal Ions and the Molecular Vibration Modes in Endohedral Dimetallofullerene La$_2$@C$_{80}$

Hidekazu Shimotani,*,†,‡ Takayoshi Ito,§ Yoshihiro Iwasa,*,†,‡ Atsushi Taninaka,||
Hisanori Shinohara,|| Eiji Nishibori,⊥ Masaki Takata,⊥,# and Makoto Sakata⊥

*Contribution from the Institute for Materials Research, Tohoku University,
Sendai 980-8577, Japan, CREST, Japan Science and Technology Corporation,
Kawaguchi 330-0012, Japan, Japan Advanced Institute of Science and Technology,
Tatsunokuchi, Ishikawa 923-1292, Japan, Department of Chemistry & Institute for Advanced
Research, Nagoya University, Nagoya 464-8602, Japan, Department of Applied Physics,
Nagoya University, Nagoya 464-8603, Japan, and JASRI-SPring-8,
Koto 1-1, Hyogo 679-5198, Japan*

Received August 29, 2003; E-mail: shimo@imr.edu (H.S.); iwasa@imr.edu (Y.I.)

Abstract: The configuration of La ions of La$_2$@C$_{80}$ in the [80]fullerene cage was investigated by use of quantum chemical calculations. We found that the D_{3d} configuration is the global minimum in total energy, being more stable by 1.9 kcal/mol than the D_{2h} configuration, which has been considered to be the most stable. The potential energy surface calculation clarified that La ions travel between 10 equivalent D_{3d} positions through D_{2h} positions and consequently form pentagonal dodecahedral trajectory, which is in good agreement with the previous synchrotron radiation structural study. The experimental and theoretical investigation of the Raman spectrum revealed that the symmetry of molecular vibration is dramatically reduced simply by encapsulation of two La ions, and resulting vibrational modes were successfully assigned. The Raman peak at 163 cm^{-1} was interpreted as the in-phase synchronously coupled mode of the [80]fullerene cage elongation and the La−La stretching, rather than a conventional and naive assignment as a metal-to-cage vibration mode.

Introduction

Various attempts have been carried out to produce, isolate, and characterize many kinds of metallofullerenes in recent years. From the primary stage of the research on fullerenes, they were expected to encapsulate atoms in their hollow inner space and consequently change their physical properties. In fact, many investigations have revealed that one or more atoms of several kinds can be encapsulated in fullerene cages. Furthermore, the differences of their properties from hollow fullerenes have been demonstrated by many investigations. The productions, isolations, and characterizations of metallofullerenes have been summarized in a recent review.[1] What make metallofullerenes unique are the variety, charge transfer, and movement of encapsulated elements. For all known metallofullerenes, encapsulated atoms are located at off-centered positions. These encapsulated metals even move inside cages, as suggested by several experiments.[2,3] Also, a recent experiment indicated that

the encapsulated atoms can participate in the electrical conduction in solid state.[4] These features imply that the location, motion, and the electronic states of encapsulated atoms are crucial issues for the investigations of metallofullerenes.

Among the vast variety of endohedral fullerenes, La$_2$@C$_{80}$, which was first reported in 1991[5,6] followed by a finding of relatively high abundance in 1995,[7] is one of the most intriguing molecules. Of particular interest is its icosahedral cage symmetry (abbreviated as I_h), which is identical to that of well-known [60]fullerene. The I_h symmetry of La$_2$@C$_{80}$ was first observed in a nuclear magnetic resonance (NMR) experiment.[8] The I_h symmetry of the [80]fullerene cage was unambiguously confirmed by the MEM/Rietveld analysis (a self-consistent iterative analysis of a combination of the maximum entropy method

---

† Tohoku University.
‡ CREST, Japan Science and Technology Corporation.
§ Japan Advanced Institute of Science and Technology.
|| Department of Chemistry & Institute for Advanced Research, Nagoya University.
⊥ Department of Applied Physics, Nagoya University.
JASRI-SPring-8.
(1) Shinohara, H. *Rep. Prog. Phys.* **2000**, *63* 843.
(2) Nishibori, E.; Takata, M.; Sakata, M.; Tanaka, H.; Hasegawa, M.; Shinohara, H. *Chem. Phys. Lett.* **2000**, *330*, 497.

(3) Nishibori, E.; Takata, M.; Sakata, M.; Taninaka, A.; Shinohara, H. *Angew. Chem., Int. Ed.* **2001**, *40*, 2998.
(4) Kobayashi, S.; Mori, S.; Iida, S.; Ando, H.; Takenobu, T.; Taguchi, Y.; Fujiwara, A.; Taninaka, A.; Shinohara, H.; Iwasa, Y. *J. Am. Chem. Soc.* **2003**, *125*, 8116.
(5) Alvarez, M. M.; Gillan, E. G.; Holczer, K.; Kaner, R. B.; Min, K. S.; Whetten, R. L. *J. Phys. Chem.* **1991**, *95*, 10561.
(6) Yeretzian, C.; Hansen, K.; Alvarez, M. M.; Min, K. S.; Gillan, E. G.; Holczer, K.; Kaner, R. B.; Whetten, R. L. *Chem. Phys. Lett.* **1992**, *196*, 337.
(7) Suzuki, T.; Maruyama, Y.; Kato, T.; Kikuchi, K.; Nakao, Y.; Achiba, Y.; Kobayashi, K.; Nagase, S. *Angew. Chem., Int. Ed. Engl.* **1995**, *34*, 1094.
(8) Akasaka, T.; Nagase, S.; Kobayashi, K.; Wälchli, M.; Yamamoto, K.; Funasaka, H.; Kako, M.; Hoshino, T.; Erata, T. *Angew. Chem., Int. Ed. Engl.* **1997**, *36*, 1643.
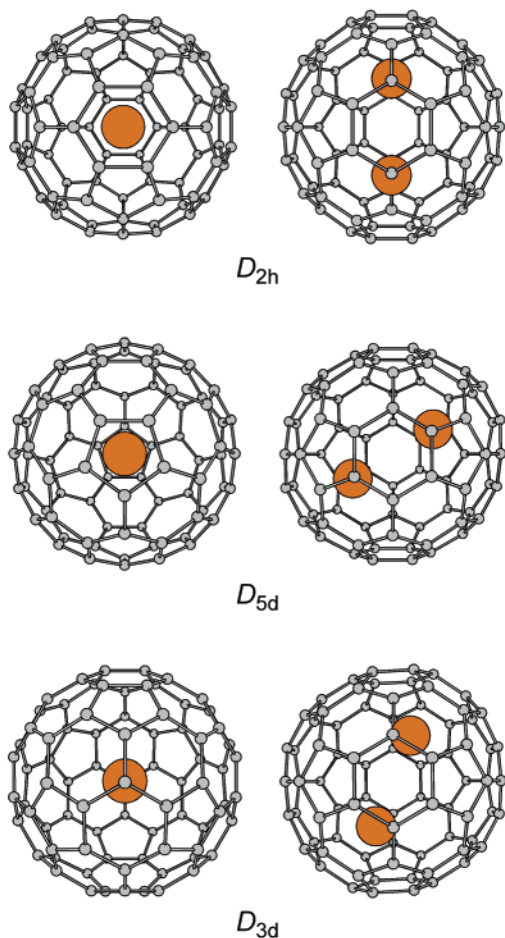
Figure 1. Three stationary points of La$_2$@C$_{80}$. Left diagrams are the views from the main axes, and right ones are the views from the six-membered rings perpendicular to the main axes.

Figure 2. MEM charge densities of the encapsulated La$_2$ pair as the equal density (1.7 eÅ^{-3}) along the (a) S_{10} and (b) C_2 axes. The model of I_h [80]fullerene cage is represented by green sticks.

(MEM) and Rietveld analysis)[9] of the high-resolution X-ray powder diffraction data.[3] The I_h [80]fullerene cage is unstable in the neutral state because of its open shell configuration. According to the theoretical calculation by Kobayashi et al.,[10] this I_h cage structure is stabilized by the six-electron transfer from the encapsulated La atoms to the cage. Thus, the electronic configuration of the molecule is expressed as $(La^{3+})_2C_{80}^{6-}$, and this electronic state is consistent with the MEM/Rietveld analysis.

The location of encapsulated La atoms is also an interesting issue. Kobayashi et al. showed that two La ions are apart from each other and located close to the interior wall of the cage.[10] The most stable La position was found on the C_2 axis, causing the symmetry reduction to D_{2h} (Figure 1 (D_{2h})). This result has been frequently used to analyze various experimental results.[3,11-13] They also calculated the electrostatic potential for La and claimed that, since the potential is very smooth, La ions are able to move around inside the cage at room temperature.[14]
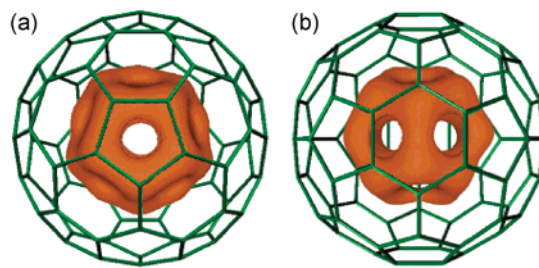
The relative positioning of the two La ions was experimentally confirmed by transmission electron microgram (TEM).[13] In the meantime, the MEM/Rietveld analysis clarified an unexpected configuration of La ions, which is displayed in Figure 2. Here, the MEM charge density of La atoms forms a dodecahedron. This image obtained from X-ray data is the average over space and time domain, in contrast to the snapshot of TEM. This La distribution indicates that the La ions are dynamically or statically disordered inside the cage, being qualitatively consistent with the prediction by Kobayashi et al. However, the pentagonal dodecahedron of La ions is not simply explained by Kobayashi's calculation because the maximum of the MEM charge density is located under the carbon atoms shared by three six-membered rings, but not under the center of six-membered rings predicted by Kobayashi et al. This inconsistency between the MEM charge density and the D_{2h} structure might suggest that La configuration needs to be considered more precisely.

Another motivation for revisiting the molecular structure comes from the spectroscopic data, such as Raman scattering and infrared (IR) absorption spectra. The IR data in the early stage was explained in terms of the I_h [80]fullerene cage,[15] while the recently carried out Raman spectra clearly show the reduction of the molecular symmetry.[11] The spectroscopic data should be useful to detect the symmetry reduction of molecules because the spectroscopy is a kind of snapshot of molecular vibration in the corresponding time scale. The comparison of the experimental data with the calculated spectra provides important information for understanding kinetics and electronic states of La ions.

In this paper, we report theoretical investigations of energetics and frequency analysis of La$_2$@C$_{80}$. We found that the D_{3d} structure is a more stable configuration than the D_{2h} structure, which has been believed to be the global minimum, and that this structure agrees with the thus far reported experimental results, MEM charge density, and interatomic distances from the X-ray absorption fine structure (XAFS).[16] We have also measured the Raman spectra of La$_2$@C$_{80}$ and compared the spectra with the theoretical results. A vibration mode associated with the motion of La ions is unambiguously assigned.

Results and Discussion

Energetics of Stationary Points. Geometry optimization was carried out with the Hartree–Fock (HF) method employing valence double-ζ quality basis sets: 3-21G and LanL2DZ basis

(9) Takata, M.; Nishibori, E.; Sakata, M. *Z. Kristallogr.* **2001**, *216*, 71.
(10) Kobayashi, K.; Nagase, S.; Akasaka, T. *Chem. Phys. Lett.* **1995**, *245*, 230.
(11) Jaffiol, R.; Débarre, A.; Nutarelli, D.; Tchénio, P.; Taninaka, A.; Cao, B.; Okazaki, T.; Shinohara, H. *Phys. Rev. B* **2003**, *68*, 014105.
(12) Kato, T.; Okubo, S.; Matsuoka, H.; Dinse, K.-P. In *Fullerenes and Nanotubes: The Building Blocks of Next Generation Nanodevices*, Proceedings of the International Symposium on Fullerenes, Nanotubes, and Carbon Nanoclusters, Paris, France, 2003; Guldi, D. M., Kamat, P. V., D'Souza, F., Eds.; Vol. 13; The Electrochemical Society: Pennington, NJ, 2003.
(13) Smith, B. W.; Luzzi, D. E.; Achiba, Y. *Chem. Phys. Lett.* **2000**, *331*, 137.
(14) Kobayashi, K.; Nagase, S.; Akasaka, T. *Chem. Phys. Lett.* **1996**, *261*, 502.
(15) Moriyama, M.; Sato, T.; Yabe, A.; Yamamoto, K.; Kobayashi, K.; Nagase, S. *Chem. Lett.* **2000**, 524.
(16) Kubozono, Y.; Takabayashi, Y.; Kashino, S.; Kondo, M.; Wakahara, T.; Akasaka, T.; Kobayashi, K.; Nagase, S.; Emura, S.; Yamamoto, K. *Chem. Phys. Lett.* **2001**, *335*, 163.

Table 1. The Computed Relative Stabilities of Three Configurations of $La_2@C_{80}$

structure	method	relative stability[a] (kcal mol^{-1})	no. imaginary frequencies
D_{3d}	HF/DZ	0	0
D_{2h}	HF/DZ	1.9	1
D_{5d}	HF/DZ	13.0	2 (degenerated)
D_{3d}	B3LYP/DZP	0	N/A
D_{2h}	B3LYP/DZP	0.1	N/A
D_{5d}	B3LYP/DZP	11.4	N/A

[a] Difference in total energy from that of the D_{3d} configuration computed using same method.
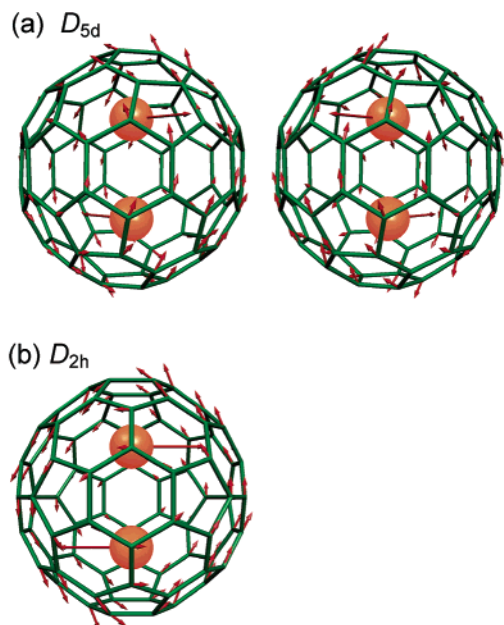
(a) D_{5d}

(b) D_{2h}

Figure 3. Vibrational modes that have an imaginary frequency for (a) D_{5d} and (b) D_{2h} configurations.

set for C atoms and La atoms, respectively. The method is hereinafter referred to as HF/DZ. First, we confirmed that the two configurations represented by the point group D_{2h} and D_{5d}, which were reported by Kobayashi et al.[10,14] (Figure 1), are indeed stationary points. The D_{5d} configuration is much higher in total energy than that of D_{2h} (Table 1), in fair agreement with Kobayashi's calculation. Here, La ions are located just under the center of five-membered rings and six-membered rings on the [80]fullerene cage for the D_{5d} and the D_{2h} configurations, respectively. To explain the experimentally obtained Raman spectra of $La_2@C_{80}$ molecules, which will be discussed in the next section, we have carried out molecular vibrational frequency analysis of these two structures with HF/DZ method. For the D_{5d} structure, we found that two modes have imaginary frequencies with the absolute value of 65 cm^{-1}. This low wavenumber indicates that this mode is related to the motion of encapsulated La ions, and in fact, the analysis showed that the mode is associated with the rotation of La ions along the inner surface of the [80]fullerene cage as depicted in Figure 3a. This imaginary frequency means that the location of La ions in the D_{5d} configuration is not stable, and in fact, this configuration is high in energy. Also, the double degeneracy of this imaginary frequency mode indicates that the D_{5d} configuration corresponds to the local maximum in energy in terms of the La positions.
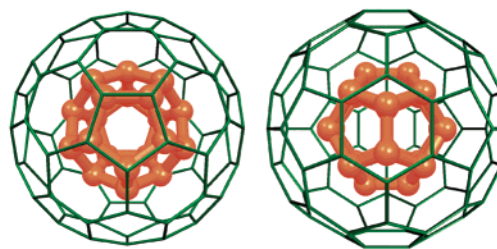
Figure 4. Ten equivalent D_{3d} positions of La atoms (orange spheres) and the energy valley path in the potential energy surface for the position of La atoms connecting the D_{3d} positions (orange bars).

We also performed a vibrational analysis of the D_{2h} configuration, which was shown to be the global minimum by Kobayashi et al. However, the frequency analysis again gave one mode with an imaginary frequency that is represented in Figure 3b. The imaginary frequency mode is also given by the frequency analysis using the Becke's three parameter functional[17] with the nonlocal correlation provided by the LYP correlation (B3LYP) method employing the same basis sets. *This means that D_{2h} is not a local minimum configuration against the movement of the La ions along the direction shown in Figure 3b.* Hence, we searched for configurations with lower total energy by shifting La ions from the D_{2h} points, and finally, we found the third stationary point with a D_{3d} point group (Figure 1), which gives the lowest total energy (Table 1). In the D_{3d} configuration, the La ions are located under the carbon atoms shared by three six-membered rings on the [80]fullerene cage, as shown in Figure 1.

In contrast to the D_{5d} structure with two degenerate modes with imaginary frequency, the D_{2d} structure has only one imaginary frequency mode shown in Figure 3b. This means that the total energy decreases when La ions are shifted from the D_{2h} position toward the D_{3d} position, while it increases upon movement of La ions toward the perpendicular directions to the $D_{2h} \rightarrow D_{3d}$ direction. This indicates that the D_{2h} configuration is a saddle point. Also, the 10 D_{3d} points, which are the equivalent global minimums in the potential energy surface, are connected along the valley of potential energy surface through the D_{2h} saddle point. Another thing to be pointed out is that the energy difference between D_{3d} and D_{2h} is only 1.9 kcal/mol, which allows the excitation of the D_{2h} configuration even at room temperature. For a more accurate comparison of the total energies of the three structures, they were re-optimized by B3LYP method with cc-pVDZ basis set in valence double-ζ with polarization quality for C atoms and LanL2DZ basis set for La atoms. The method is hereinafter referred to as B3LYP/ DZP. The total energies of the optimized structures by the B3LYP/DZP method are summarized in Table 1. The higher-level calculation gives a smaller difference of total energies (0.1 kcal mol^{-1}) between the D_{3h} and the D_{2h} structure, and the D_{3d} structure remains more stable than the D_{2h} structure. The total energy of the D_{5d} configuration is again much higher than those of the other two configurations. This result confirms the above discussions based on HF/DZ calculations. Figure 4 shows the 10 equivalent D_{3d} positions of La ions as orange spheres and the energy valley paths through a D_{2h} saddle point as orange lines. The above consideration leads us to speculate that La ions move from a D_{3d} position to another D_{3d} position through the

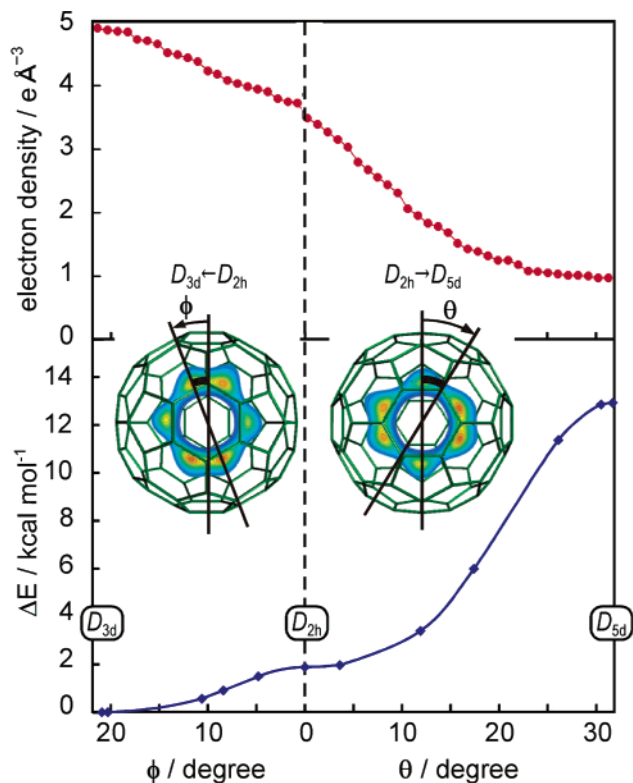(17) Becke, A. D. *J. Chem. Phys.* **1993**, *98*, 5648.

Figure 5. Experimental electron density obtained from MEM/Rietveld analysis (the upper panel) and the total energy derived by HF/DZ method (the lower panel) along the path connecting D_{3d}, D_{2h}, and D_{5d} positions of La atoms. The paths are represented by the thick arcs in inset, where definitions of θ and φ are also given.

energy path, forming a pentagonal dodecahedron of La when averaged in a long time scale. The D_{5d} configurations are scarcely excited at room temperature because of their high total energy. The trajectory of La ions represented in Figure 4 is in good agreement with the experimental MEM charge density of La₂@C80 (Figure 2), supporting our calculations.

For further examination of the potential energy surface, we have compared the total energy and the experimental electron density derived by the MEM/Rietveld method.[3] Figure 5 displays a plot of the experimental electron density and the computed total energy along a $D_{3d}-D_{2h}-D_{5d}$ path of La ions. As shown in Figure 5, the highest electron density is observed at the D_{3d} position of La atoms, which is the most stable position in the path. The total energy increases monotonically with displacement of La atoms from the D_{3d} position to the D_{5d} position through the D_{2h} saddle point. Importantly, the experimental electron density monotonically decreases as the total energy increases. The close correlation between the experimental electron density distribution and the calculated total energy shown in Figure 5 provides firm evidence for our finding of the stable D_{3d} structure.

A closer inspection of the interatomic distances also provides useful information. The computed interatomic distances for the D_{3d} and D_{2h} configurations, as well as the experimental values derived by the MEM/Rietveld method[3] and XAFS,[16] are summarized in Table 2. A significant difference between the two models is seen in the distance between La and the closest C atom, r_{La-C}. The D_{3d} configuration gives 2.467 Å, which is considerably smaller than the value of 2.573 Å for the D_{2h} configuration. This short La−C distance derived from the D_{3d}

Table 2. Selected Experimental and Theoretical Geometrical Parameters of La₂@C80

structure	method	$r_{La-La}{}^{a}$ (Å)	$r_{La-C}{}^{b}$ (Å)	reference
MEM/Rietveld		3.84(2)	2.39(3)	3
XAFS		3.90(1)	2.42(1)	16
D_{3d}	HF/DZ	3.645	2.467	this work
D_{2h}	HF/DZ	3.652	2.573	this work
D_{3d}	B3LYP/DZP	3.731	2.429	this work
D_{2h}	B3LYP/DZP	3.743	2.553	this work

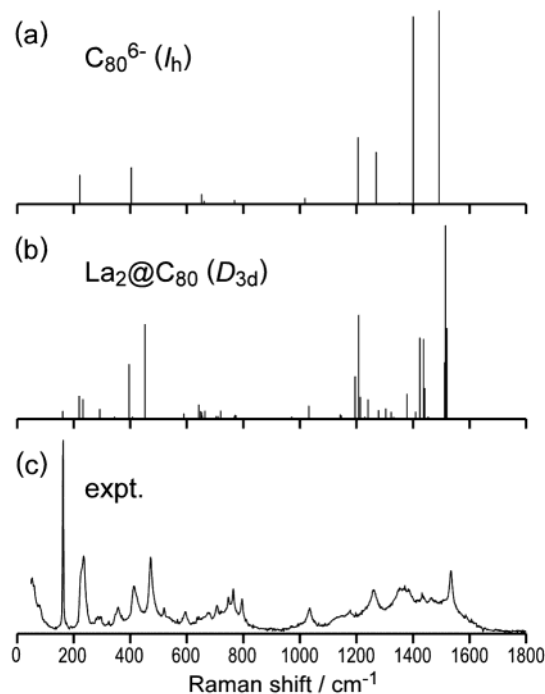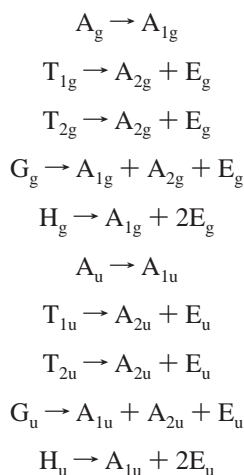*a* The distance between two La ions. *b* The distance between a La ion and the closest carbon atoms.

Figure 6. Raman spectra of (a) $C_{80}{}^{6-}$ and (b) La₂@C80 (D_{3d}) computed using the HF/DZ method and (c) the experimental Raman spectrum of La₂@C80 at room temperature.

model agrees fairly well with the experimental observations: 2.39 Å from MEM and 2.42 Å from XAFS. There is no substantial difference in the distance between two La ions of the three structures computed using the Hartree−Fock method. To improve the level of calculation, we have performed structure refinement by use of the B3LYP/DZP method. The r_{La-C} of the D_{3d} structure by the B3LYP/DZP method gave a quite close value to the experiment, and furthermore, the La−La distance, r_{La-La}, is also improved using the B3LYP/DZP method. These results strongly support the D_{3d} model rather than the D_{2h} model.

The relative stability of D_{3d} and D_{2h} configurations should be strongly dependent on the nearest La−C and La−La interactions. To have an insight into these interactions, the interatomic distances are very useful parameters. The nearest La−C distances in the D_{3d} and the D_{2h} configurations (Table 2) are shorter than the summation of van der Waals radius of C atom and Pauling's ionic radius of La³⁺ ion (1.70 + 1.15 = 2.85 Å). This indicates that the interaction between La and C involves not only attractive Coulombic interaction but also covalent interaction. Thus, the shorter La−C distance stabilizes the system. On the other hand, the La−La interaction is purely repulsive Coulomb, which stabilizes the system in case of larger La−La distance. In the derived configurations, both the shortest

La−C and La−La distances in the D_{3d} model are smaller than those in the D_{2h} configuration. Particularly, the La−C distance is 5% smaller, while the difference in the La−La distance is only 0.3%. The short La−C distance, in other words, the attractive La−C interatomic interaction might be a dominant cause for stabilization of D_{3d} configuration.

Raman Spectroscopy and Frequency Analysis. The experimental Raman spectrum of $La_2@C_{80}$ recorded at room temperature is displayed in Figure 6c. The spectrum qualitatively agrees with the recent report.[11] To understand this rich spectrum, we have computed the Raman spectra for several configurations. First, we calculated the spectra for the empty C_{80}^{6-} cage having the exact I_h symmetry by means of the HF/DZ, and its result is shown in Figure 6a. As shown in Figure 6a, because of I_h symmetry of [80]fullerene cage, only 14 modes ($3A_g + 11H_g$) are Raman active, while the C_{80}^{6-} cage has 234 vibrational modes ($3A_g + 4T_{1g} + 5T_{2g} + 8G_g + 11H_g + 1A_u + 6T_{1u} + 7T_{2u} + 8G_u + 9H_u$). The experimental spectrum (Figure 6c) shows many more peaks than expected for I_h-symmetric C_{80}^{6-}, indicating that the symmetry reduction of vibration modes is induced by the encapsulated La ions. Figure 6b shows the Raman spectrum of D_{3d}-symmetric $La_2@C_{80}$ computed at the same level of theory as I_h-symmetric C_{80}^{6-}. In case of the D_{3d} structure of $La_2@C_{80}$, the lowering of symmetry causes the splitting of degenerated vibrational modes of I_h-symmetric C_{80}^{6-} as described below:

$$A_g \rightarrow A_{1g}$$
$$T_{1g} \rightarrow A_{2g} + E_g$$
$$T_{2g} \rightarrow A_{2g} + E_g$$
$$G_g \rightarrow A_{1g} + A_{2g} + E_g$$
$$H_g \rightarrow A_{1g} + 2E_g$$
$$A_u \rightarrow A_{1u}$$
$$T_{1u} \rightarrow A_{2u} + E_u$$
$$T_{2u} \rightarrow A_{2u} + E_u$$
$$G_u \rightarrow A_{1u} + A_{2u} + E_u$$
$$H_u \rightarrow A_{1u} + 2E_u$$

The splitting causes the complicated spectrum in Figure 6b, which shows qualitative agreement with the experimental data (Figure 6c), particularly in the wavenumber region below 500 cm^{-1}.

Another feature to be noted is the coupling of the La ions' motion with the cage vibrations, which results in additional vibrational modes. Figure 7 represents an example of the splitting of degenerate modes and the coupling of La and cage vibrational modes. The H_g mode of C_{80}^{6-} with the lowest computed wavenumber splits into three modes: one nondegenerate A_{1g} mode and two doubly degenerate E_g modes. The atomic motions for the latter two E_g modes are displayed in Figure 7c−f. The A_{1g} mode corresponding to the vibration that elongates the [80]fullerene cage has z^2-type symmetry. Here, the definition of the z direction is parallel to the C_3 axis connecting two La ions. The mode is coupled with La−La stretching modes (A_{1g}), resulting in two A_{1g} vibrational modes
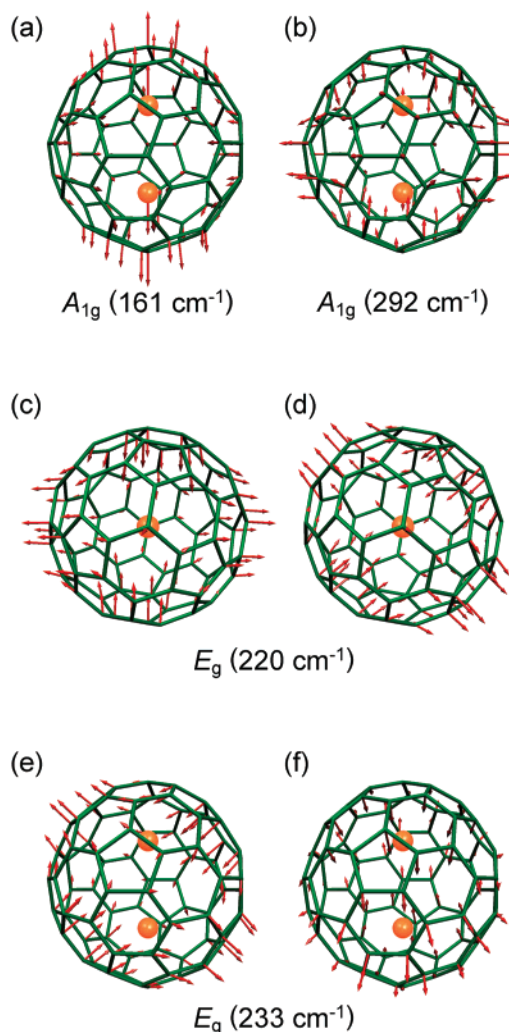

Figure 7. Vibrational modes of $La_2@C_{80}$ that originate from the E_g mode of C_{80}^{6-}, having the lowest computed wavenumber. The irreducible representations and computed wavenumbers are (a) A_{1g}, 161 cm^{-1}, (b) A_{1g}, 292 cm^{-1}, (c,d) E_g, 220 cm^{-1}, and (e,f) E_g, 233 cm^{-1}, respectively.

(Figure 7a,b). These two modes correspond to in-phase and antiphase combinations of the vibrational modes, respectively. Figure 8 shows the calculated and experimental Raman spectra displaying the splitting of degenerated H_g mode at 222 cm^{-1} for C_{80}^{6-} and the coupling of La ions' motion with [80]fullerene cage vibrations. The H_g mode splits into the $2A_{1g} + 2E_g$ modes, as shown in Figure 7, in the case of $La_2@C_{80}$ (D_{3d}). Among the resulting four modes, one A_{1g} mode computed to be 292 cm^{-1} is outside the range of Figure 8. The computed wavenumbers of the three vibrational modes agree well with experimental values. Hence, the peak at 162.8 cm^{-1} is assigned as the in-phase combination of the La−La stretching mode with the vibrational mode elongating the [80]fullerene cage (Figure 7a). It is well-known that a Raman peak is also observed in the same wavenumber region in several monometallofullerenes $M@C_{82}$ (M = La, Y, Ce, Gd) and was assigned as the relative motion of encapsulated metal ions and carbon cage.[18,19] In contrast to this naive assignment, it was found that the

(18) Lebedkin, S.; Renker, B.; Heid, R.; Schober, H.; Rietschel, H. *Appl. Phys. A* **1998**, *66*, 273.
(19) Krause, M.; Hulman, M.; Kuzmany, H.; Dennis, T. J. S.; Inakuma, M.; Shinohara, H. *J. Chem. Phys.* **1999**, *111*, 7976.
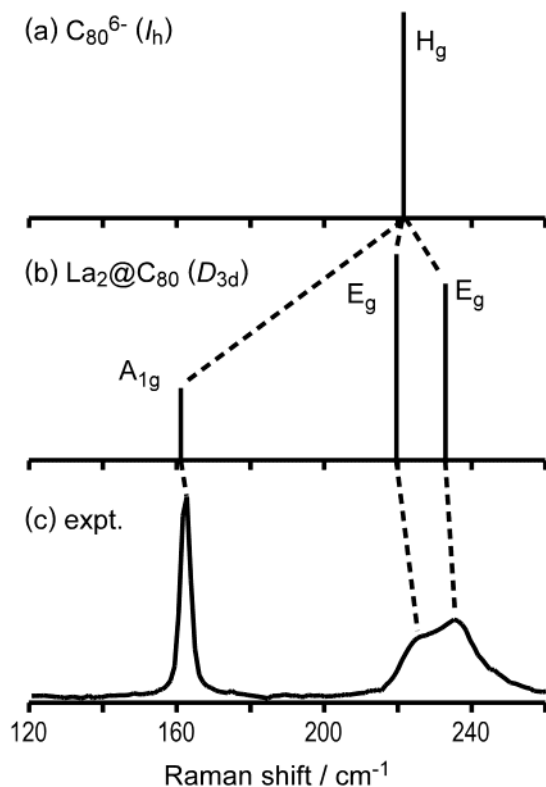
Figure 8. Low wavenumber region of the Raman spectra of (a) C_{80}^{6-} (computed), (b) D_{3d}-symmetric La$_2$@C$_{80}$ (computed), and (c) La$_2$@C$_{80}$ (experimental).

corresponding mode in La$_2$@C$_{80}$ should be interpreted as the totally symmetric mode described in Figure 7a.

Conclusions

The potential energy surface of La$_2$@C$_{80}$ for the La atoms position in the [80]fullerene cage was examined. We found that the most stable configuration is D_{3d}, and that the D_{2h} configuration, which was reported to be the lowest in energy,[14] is the saddle point. Since the energy difference between the D_{3d} configuration and the D_{2h} configuration is only 1.9 kcal/mol, which is empirically low enough to be excited at room temperature, La atoms possibly move between 10 equivalent D_{3d} configurations through intervening D_{2h} configuration. The model shows a fair agreement with the MEM electron density[3] and the experimental La−C distances derived by both MEM/ Rietveld method[3] and XAFS.[16]

We have also calculated the Raman spectra for the I_h-symmetric [80]fullerene and the D_{3d}-symmetric La$_2$@C$_{80}$ and compared them with the experimental observations. The encapsulation of two La ions induces considerable splitting of

Raman peaks despite the unchanged cage structure and qualitatively explains the observed Raman spectra. The coupling of a La−La stretching mode and a [80]fullerene cage vibrational mode was found in the wavenumber region below 300 cm^{-1}, and some peaks were successfully assigned by taking the splitting and coupling of the modes into account.

Experimental Section

Theoretical Calculations. All calculations were made using Gaussian 98[20] on VT-SuperCluster XA series (Visual Technology, Inc.) using four parallel Alpha21264 CPUs. A geometry optimization takes 1 or 2 days with the system. For geometry optimizations, frequency analyses, and potential energy calculations, the Hartree−Fock method with valence double-ζ quality basis sets for both C atoms (3-21G) and La atoms (LanL2DZ) was employed. The method is referred to as HF/DZ in this paper. The geometry optimization and the frequency analysis of the D_{2h} configuration were repeated using B3LYP method with same basis sets. The geometries of the D_{3d} and D_{2h} configurations were also optimized by B3LYP method with cc-pVDZ basis set in valence double-ζ with polarization quality for C atoms and LanL2DZ basis set for La atoms. Pure d functions were employed for the calculations. The method is referred to as B3LYP/DZP. All wave functions were tested their stabilities by "Stable" keyword of Gaussian 98 within the restricted Hartree−Fock or B3LYP method with real wave functions. Frequency analyses were performed by analytic evaluation of the second derivative of the energy with respect to nuclear displacement. The computed wavenumbers were scaled by 0.9085.[21]

In the calculations of potential energy surface, La$_2$@C$_{80}$ was restricted to C_{2h} symmetry. The geometrical parameters were fully optimized using HF/DZ method except for the rotation angle of the La−La axis from the D_{2h} configuration. The computed total energies at the various rotation angles were plotted as a function of the rotation angle.

Raman Spectroscopy. La$_2$@C$_{80}$ purified with HPLC was dissolved in carbon disulfide and was deposited on a glass substrate coated with gold. The deposited sample was measured with a micro Raman spectrometer. The wavelength of exciting laser was 632.8 nm.

(20) Frisch, M. J.; Trucks, G. W.; Schlegel, H. B.; Scuseria, G. E.; Robb, M. A.; Cheeseman, J. R.; Zakrzewski, V. G.; Montgomery, J. A., Jr.; Stratmann, R. E.; Burant, J. C.; Dapprich, S.; Millam, J. M.; Daniels, A. D.; Kudin, K. N.; Strain, M. C.; Farkas, O.; Tomasi, J.; Barone, V.; Cossi, M.; Cammi, R.; Mennucci, B.; Pomelli, C.; Adamo, C.; Clifford, S.; Ochterski, J.; Petersson, G. A.; Ayala, P. Y.; Cui, Q.; Morokuma, K.; Malick, D. K.; Rabuck, A. D.; Raghavachari, K.; Foresman, J. B.; Cioslowski, J.; Ortiz, J. V.; Stefanov, B. B.; Liu, G.; Liashenko, A.; Piskorz, P.; Komaromi, I.; Gomperts, R.; Martin, R. L.; Fox, D. J.; Keith, T.; Al-Laham, M. A.; Peng, C. Y.; Nanayakkara, A.; Gonzalez, C.; Challacombe, M.; Gill, P. M. W.; Johnson, B. G.; Chen, W.; Wong, M. W.; Andres, J. L.; Head-Gordon, M.; Replogle, E. S.; Pople, J. A. *Gaussian 98*, revision A.11.1; Gaussian, Inc.: Pittsburgh, PA, 1998.
(21) Scott, A. P.; Radom, L. *J. Phys. Chem.* **1996**, *100*, 1652.